

Accepted Manuscript

New somatostatin-drug conjugates for effective targeting pancreatic cancer

E. Ragozin, A. Hesin, A. Bazylevich, H. Tuchinsky, A. Bovina, T. Shekhter Zahavi, M. Oron-Herman, G. Kostenich, M.A. Firer, T. Rubinek, I. Wolf, G. Luboshits, M.Y. Sherman, G. Gellerman

PII: S0968-0896(18)30710-7
DOI: <https://doi.org/10.1016/j.bmc.2018.06.032>
Reference: BMC 14424

To appear in: *Bioorganic & Medicinal Chemistry*

Received Date: 10 April 2018
Revised Date: 14 June 2018
Accepted Date: 24 June 2018

Please cite this article as: Ragozin, E., Hesin, A., Bazylevich, A., Tuchinsky, H., Bovina, A., Zahavi, T.S., Oron-Herman, M., Kostenich, G., Firer, M.A., Rubinek, T., Wolf, I., Luboshits, G., Sherman, M.Y., Gellerman, G., New somatostatin-drug conjugates for effective targeting pancreatic cancer, *Bioorganic & Medicinal Chemistry* (2018), doi: <https://doi.org/10.1016/j.bmc.2018.06.032>

This is a PDF file of an unedited manuscript that has been accepted for publication. As a service to our customers we are providing this early version of the manuscript. The manuscript will undergo copyediting, typesetting, and review of the resulting proof before it is published in its final form. Please note that during the production process errors may be discovered which could affect the content, and all legal disclaimers that apply to the journal pertain.



New somatostatin-drug conjugates for effective targeting pancreatic cancer.

Ragozin E.,^{1#} Hesin A.,^{2,3#} Bazylevich A.,¹ Tuchinsky H.,⁴ Bovina A.,¹ Shekhter Zahavi T.,⁵ Oron-Herman M.,⁶ Kostenich G.,⁶ Firer M.A.,⁷ Rubinek T.,^{2,3} Wolf I.,^{2,3} Luboshits G.,⁷ Sherman M.Y.⁴ and Gellerman G.^{1*}

¹ Department of Chemical Sciences, Ariel University, Ariel, 40700, Israel

² The Oncology Institute, Tel Aviv Souraski Medical Center, Tel-Aviv, 62431, Israel

³ Sackler Faculty of Medicine, Tel-Aviv University, Tel-Aviv, 69978, Israel

⁴ Department of Molecular Biology, Ariel University, Ariel, 40700, Israel

⁵ The Department of Molecular Microbiology and Biotechnology, George S. Wise Faculty of Life Sciences, Tel-Aviv University, Tel-Aviv, 69978, Israel

⁶ The Advanced Technologies Center, Sheba Medical Center, Tel Hashomer, 52621, Israel

⁷ Department of Chemical Engineering, Ariel University, Ariel, 40700, Israel

Equal contribution

Address for correspondence

Prof. Gary Gellerman,

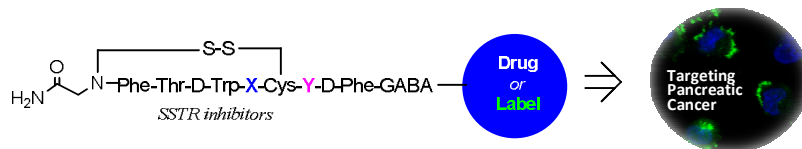
Dept. Chemical Sciences,

Ariel University, Ariel 40700, Israel

Email: garyg@ariel.ac.il

ACCEPTED MANUSCRIPT

Graphical Abstract



Abstract

Pancreatic cancer poorly responds to available drugs, and finding novel approaches to target this cancer type is of high significance. Here, based on a common property of pancreatic cancer cells to express somatostatin receptors (SSTR), we designed drug conjugates with novel somatostatin-derived cyclic peptides (SSTp) with broad selectivity towards SSTR types to facilitate drug targeting of the pancreatic cancer cells specifically. Uptake of our newly designed SSTps was facilitated by SSTRs expressed in the pancreatic cancers, including SSTR2, SSTR3, SSTR4 and SSTR5. Three major drugs were conjugated to our best SSTps that served as delivery vehicles, including Camptothecin (CPT), Combretastatin-4A (COMB) and Azatoxin (AZA). All designed drug conjugates demonstrated penetration to pancreatic cancer cell lines, and significant toxicity towards them. Furthermore, the drug conjugates specifically accumulated in tumors in the animal xenograft model, though some accumulation was also seen in kidney. Overall these findings lay the basis for development of novel drug series that could target the fatal pancreatic cancer.

Keywords: SSTR; peptide conjugate; targeted drug delivery; pancreatic cancer; SPPS; stability profiles.

Abbreviations

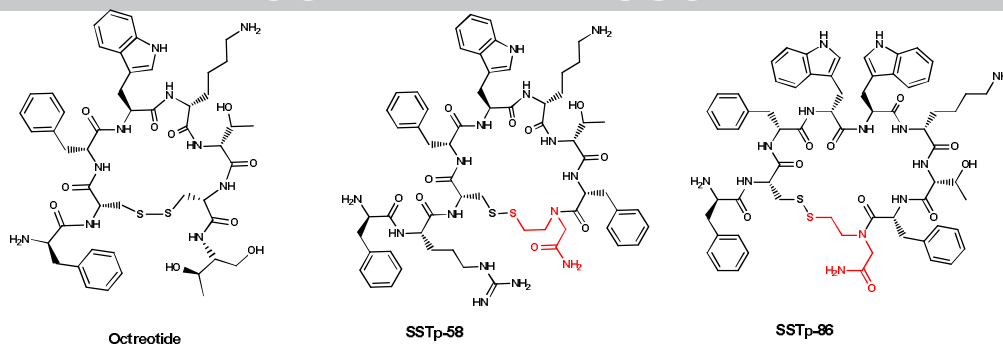
ACN – Acetonitrile; **cAMP** – 3',5'-cyclic adenosine monophosphate; **DCM** – Dichloromethane; **DIPEA**-Diisopropylethylamine; **DMAP** - 4-*N,N*-(dimethylamino)pyridine; **DMBA** – Dimethyl barbituric acid; **DMF** - *N,N*dimethylformamide; **DMSO** - Dimethyl sulfoxide; **Fmoc** - 9-fluorenylmethoxycarbonyl; **HPLC** - High-pressure liquid chromatography; **LC-MS** - liquid chromatography-mass spectroscopy; **MALDI** - Matrix-assisted laser desorption/ionization; **PyBOP** - Benzotriazol-1-yl-oxytripyrrolidino-phosphonium hexafluorophosphate; **rpm** - rounds per minute; **SST** – somatostatin; **TFA** - Trifluoroacetic acid; **TIPS** – Triisopropylsilane; **XTT** - 2,3-bis(2-methoxy-4-nitro-5-sulfohenyl)-5-[(phenylamino) carbonyl]-2H-tetrazolium hydroxide

1. Introduction

Pancreatic cancer is the most lethal gastrointestinal cancer. The disease is usually diagnosed at advanced metastatic stages, it responds poorly to chemotherapeutics and has an overall 5-year survival rate between 6-37% [1]. Because of such medical urgency, selective drug delivery to pancreatic cancer using small molecules [2] proteins [3], nanoparticles [4-7], liposomes [8, 9], quantum dot [10] and micelles [11, 12] has been developed. However, the progress in the field has not led so far to dramatic breakthrough in patient treatments.

During the last 20 years there has been a substantial effort to target receptors overexpressed in cancer cells [13], in order to achieve specific receptor-mediated endocytotic delivery of drugs [14-17]. Since somatostatin is a natural peptide hormone, a somatostatin receptor family (SSTRs) constituting of 5 subtypes (SSTR 1-5), has drawn attention of medicinal chemists as promising targets for peptide-based targeted drug delivery [18]. SSTRs are heterogeneously expressed in the human gastrointestinal tumors, including pancreatic and neuroendocrine pancreatic cancer, and intratumoral vessels, and often multiple SSTR subtypes can co-express in the same cell [19-24]. So far, the most useful peptide developed as a drug carrier for SSTR overexpressed malignancies has been the modified (linker armed) S-S-bridged octapeptide octreotide (sandostatin) that preferentially targets SSTR2 [25], though it also has a significant affinity towards SSTR3 and SSTR5. Several drug conjugates based on octreotide have been reported for pancreatic cancer, including camptothecin (CPT) [26] and doxorubicin [27] conjugates. These conjugates displayed significant antitumor activities against pancreatic cancers and reduced toxicity to benign tissues. However, existing peptides show significant specificity towards different SSTR types, which may narrow their use to cancers that express only these receptor types. Our goal was to develop peptides with broad specificity as vehicles for targeting drugs to pancreatic cancers.

Here we report synthesis of novel conjugates comprising cyclic peptides SSTp-58 and SSTp-86 that are based on the sandostatin motive and incorporating the S-S-bridged backbone GlyS2 building unit introduced at the beginning of the assembly [28]. Previous *in vivo* studies of tumor targeting by SSTp-86 revealed its selective accumulation in HT-29 colon (expressing SSTR3 and SSTR5) and H69 SCLC xenografts (expressing SSTR2) [29-32].



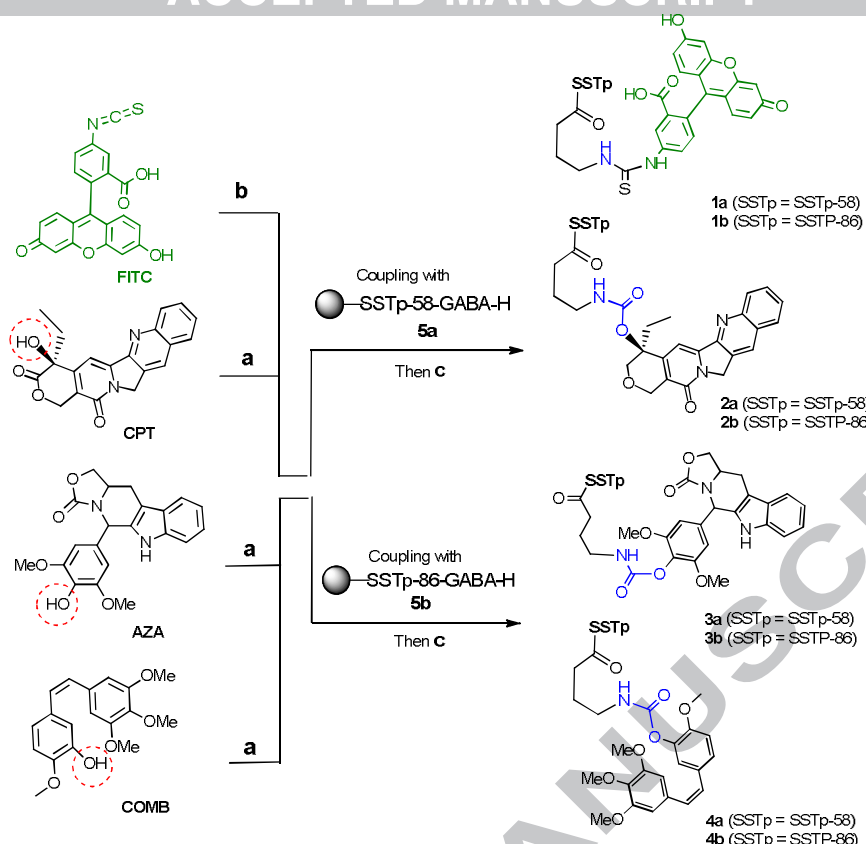
Scheme 1. Structures of SSTp-58, SSTp-86 and octreotide

Here, we constructed drug conjugates with SSTp-58 and SSTp-86 peptides, and investigated their antitumor activities with pancreatic cancer models. We found that these drug conjugates effectively and specifically penetrated pancreatic cancer cells, depending of expression of a broad range of SSTRs, and accumulated in the pancreatic tumors in a xenograft model. Tumor growth inhibition, maintenance of body weight and overall survival of pancreatic xenograft models are currently under investigation in our lab.

2. Results and Discussion

2.1 Synthesis of SSTp - mono drug or fluorescein conjugates 1-4, SSTp-dual drug and fluorescein conjugates 7

Several peptide–drug conjugates **1-4** employing analogs of the SSTp 58 and -86 peptides as targeting moiety (Scheme 2), were synthesized using solid phase organic synthesis (SPOS). Mono conjugates of SSTp-86 bearing fluorescein (**1b**), CPT (**2b**) and COMB (**4b**) have been synthesized and characterized previously [35]. The SSTp-58-fluorescein (**1a**) was synthesized in the same manner as for **1b**. In general, the fully protected cyclic peptide SSTp-58 (**5a**) and SSTp-86 (**5b**) with GABA linker (Scheme 2) were synthesized on an acid-labile Rink amide MBHA resin (substitution level, 0.56 mmol/g, 1g) using standard Fmoc solid-phase peptide synthesis (SPPS) by following a published procedure [28].



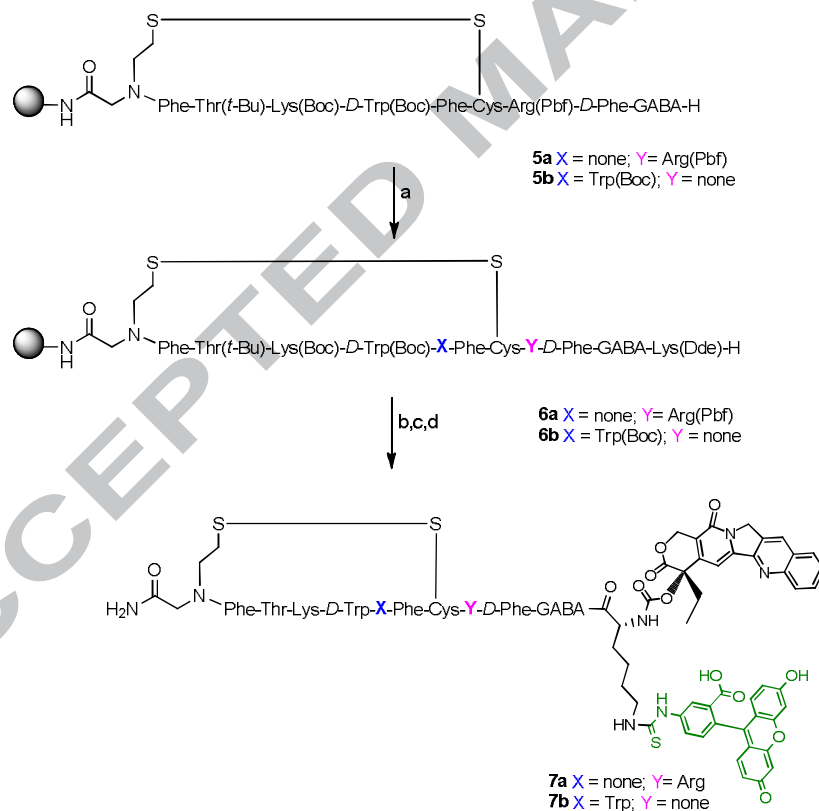
a. (i) 4-Nitrophenyl chloroformate, pyridine, 90°C, 1h; (ii) DMAP (6eq.) DCM, 0°C; b. DIEA, DMF, rt; c. 95:2.5:2.5 TFA/TIS/H₂O, 0°C then rt, 1h.

Scheme 2. Synthesis of peptide conjugates **1a** – **4b**.

As stated above, we decided to develop peptide-drug conjugates with broad specificity than octreotide as peptide vehicle for targeting drugs to pancreatic cancers. To synthesize conjugates **2** - **4**, first the N-terminal Fmoc group of the GABA linker of preloaded SSTp-58 and -86 respectively was removed (20% piperidine in NMP, 10 mL) releasing the primary amine toward **5a** or **5b** correspondingly. Consequently, activated CPT, AZA, and COMB (CPT, AZA, or COMB [3 eq.], 4-nitrophenyl chloroformate [3 eq.], pyridine, 90°C, 1 h; then DMAP [6 eq.] DCM, 0°C) were reacted with the primary amine, providing conjugates **2a,b**, **3a,b** and **4a,b** with an aliphatic and aromatic carbamate conjugation site, respectively. Finally, the on-resin-synthesized conjugates were cleaved from the solid support (cold, 95:2.5:2.5 TFA/TIS/H₂O, room temperature, 1h), precipitated by diethyl ether, purified by preparative HPLC, and characterized by MS (supporting information material). Hetero-nuclear peptide drug conjugates **7a,b** were assembled on Rink amide MBHA resin similarly to mono-conjugates **2-4** accept the introduction of split functional orthogonally protected tail Fmoc-

Lys(Dde)-OH [11] (Scheme 3). First, on-resin intermediates **6a-b** with deprotected Lys split functional tail were obtained after Fmoc removal of their precursors (20% piperidine in NMP, 10 mL). At this stage, the cyclic SSTp targeting carrier peptides were adapted for double drug conjugation of CPT and FITC. Notably, in its free form, CPT in particular is very potent but it has poor solubility and produces off-target cytotoxicity, factors that have precluded its clinical development. We hypothesized that in general, conjugation of CPT to a targeting peptide would improve its pharmacological properties.

Initially, the free *N*-terminus amine of the resulting **6a** and **6b** were loaded with activated CPT (CPT [3 eq.], 4-nitrophenyl chloroformate [3 eq.], pyridine, 90°C, 1 h; then DMAP [6 eq.] DCM, 0°C) leading to creation of biodegradable carbamate linkage. Then the second protecting group Dde was also removed (2% hydrazine in DMF, 3 min (x 3)) and the primary ω-amine of Lys was allowed to react with FITC (FITC [1.5 eq.], DIEA [3 eq.] in DMF). Finally, all the on-resin synthesized conjugates were cleaved from the solid support and precipitated by the addition of cold diethyl ether, isolated, lyophilized and identified by LC-MS and HRMS as dual conjugates **7a-b**.



a. (i) Fmoc-Lys(Dde)-OH, PyBoP, DIEA, DMF, rt; (ii) 20% Piperidine in DMF; b. (i) CPT, 4-Nitrophenyl chloroformate, pyridine, 90°C, 1h; (ii) DMAP (6eq.) DCM, 0°C; c. 2% hydrazine in DMF, 3 min. (x 3); d. DIEA, DMF, rt; e. 95:2.5:2.5 TFA/TIS/H₂O, 0°C then rt, 1h.

Scheme 3. Synthesis of hetero-nuclear conjugates **7a**, **7b** with FITC and CPT

2.2 Receptor type specificity of SSTp-drug conjugates.

In order to explore the targeting properties of STTs we established *in vitro* model using subclones of HEK-293 cells each overexpressing a single SSTR subtype. Though pancreatic cancer cell lines mostly express SSTR2 and SSTR5 receptors, human pancreatic tumors can also express other SSTRs [22, 23]. Here we assess the role of all five SST receptor subtypes in binding and transport of our novel peptides to cells. First, we tested the ability of peptides **1a** and **1b** to inhibit the cAMP signaling pathway activity in a receptor-mediated manner via G-protein coupled mechanism [37, 39, 40]. cAMP signaling pathway activity was assessed using a reporter gene system of cAMP response element (CRE) fused to firefly luciferase, where CRE promoter activity reflects intracellular cAMP accumulation level [36, 41, 42]. First, we calibrated the system using native somatostatin SST-14 and the SSTR 2, 3, 5-selective agonist octreotide [25]. As expected, SST-14 inhibited the CRE promoter activity in SSTR 1-5 transfected cells, whereas octreotide inhibited the CRE promoter activity in SSTR 2, 3 and 5-transfectants selectively (Fig. S-1, also see supplementary info). In this assay, peptide **1a** was less potent than **1b** in cells transfected with SSTR5 or SSTR4, while in cells expressing SSTR2 or SSTR3, they demonstrated similar suppression of CRE promoter. Neither of the tested peptides was effective in inhibition of the cAMP signaling pathway activity in SSTR1-transfectants (Fig. 1).

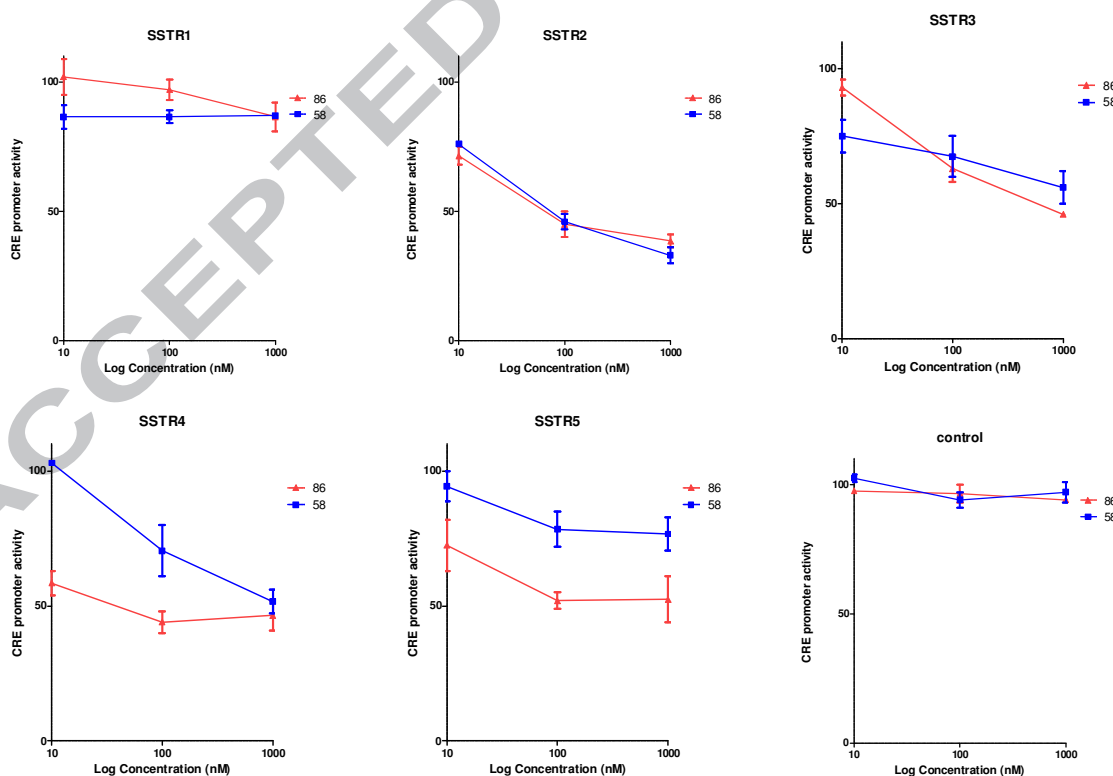


Figure 1: Inhibition of the CRE promoter activity by **1a** and **1b**. HEK-293 cells were transfected with a

plasmid encoding reporter luciferase gene under the control of the cAMP response element (CRE), and co-transfected with SSTR 1-5 expression vectors or with empty vector. After 1 day cells were treated with FSK or FSK plus SST analog **1a** or **1b**, and CRE promoter activity was evaluated by monitoring luminescence. Results are given as mean \pm SD of at least three independent experiments.

To further study the receptor specificity, we examined the build-up of **1b** in HEK-293 cells over-expressing SSTR 1- 5 and found remarkable accumulation in all-transfectants, except for SSTR1 (Fig. 2). These data indicate strong receptor-specific accumulation of the peptides in cells, and a broad specificity towards the SSTR types, which justifies using these moieties as vehicles for specific drug delivery to pancreatic cancers that express various SSTRs.

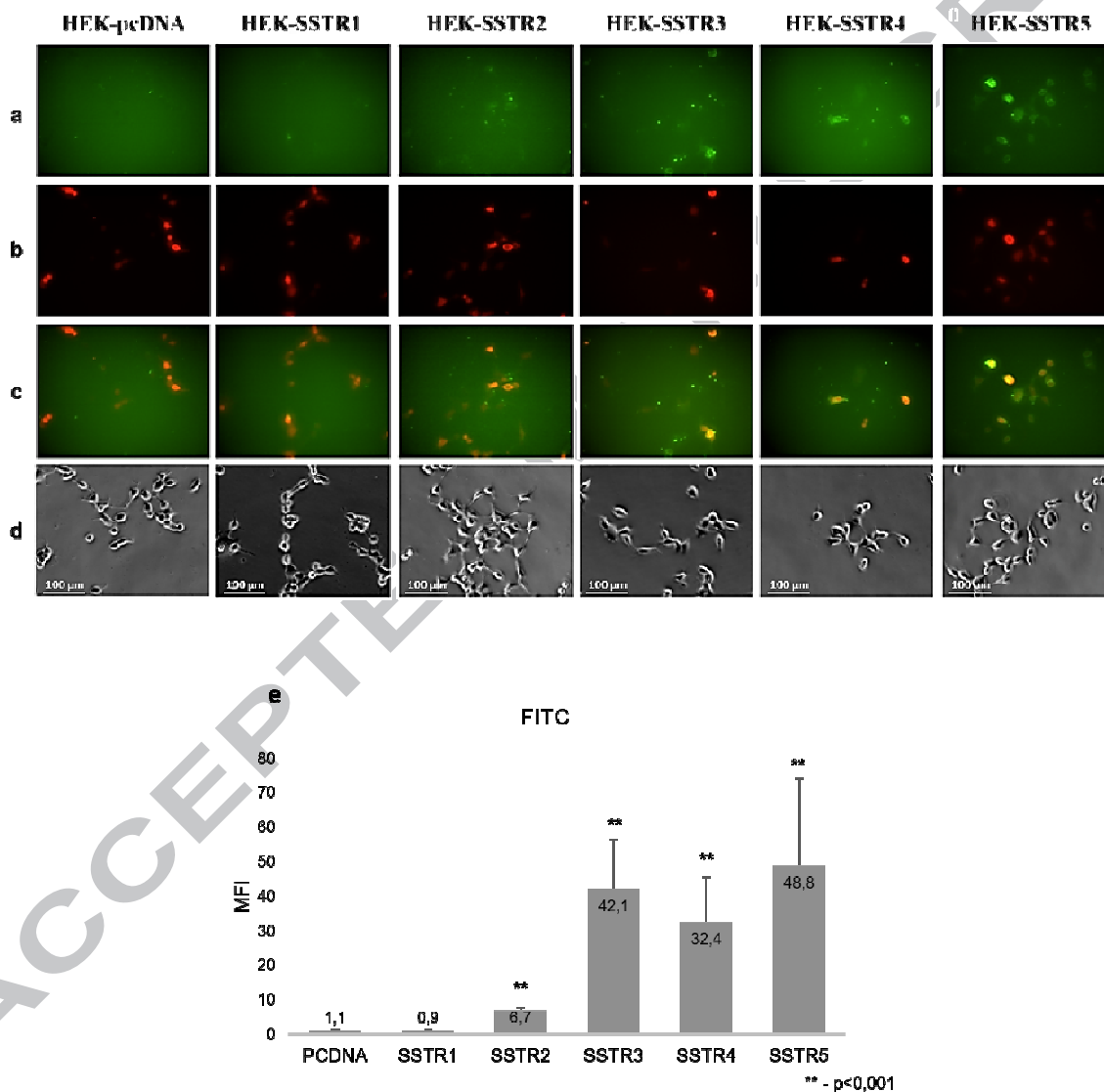
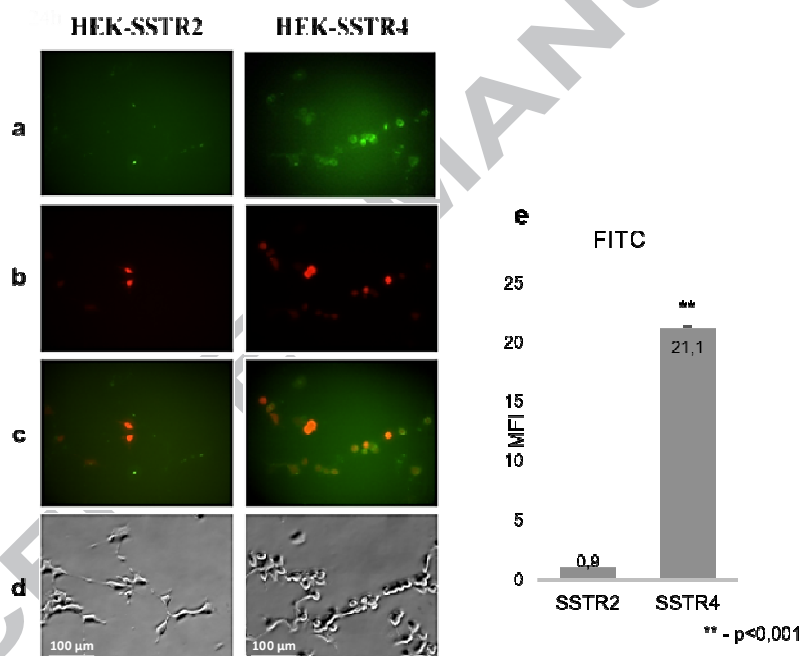


Figure 2: Accumulation of **1b** in SSTR-transfected HEK-293: HEK-293 cells were transfected with SSTR 1-5 expression vectors or control empty vector and co-transfected with RFP expression vector to identify transfected cells. 48 hours later 400 nM **1b** was added for 30 minutes, and both FITC (**1b** contains FITC moiety) (a) and RFP (b) fluorescence were monitored. (c) Merged RFP and FITC images. Phase-contrast imaging (d) shows total cell number in the samples. (e) Histogram showing quantitative image analysis of the fluorescence intensity of FITC⁺ cells (mean \pm SD; n = 10). The

numbers denote mean fluorescence intensity (MFI). Data are representative of three independent experiments ($P < 0.001$).

In further confirm binding specificity in our receptor transfection protocol, we chose **1b** to conduct a competition assay against octreotide, which effectively binds SSTR2, but not SSTR4 (Fig. 3) [25]. The concentrations of the peptides in this experiment were 400 nM for **1b** and 800 nM for octreotide. As shown in Figure 3, octreotide competed with **1b** in SSTR2 transfected cells, but not in the SSTR4-transfectants, indicating strong receptor specificity of peptides in our assay. Together, data on the effects of **1a** and **1b** on activity of receptors and receptor-specific penetration into cells suggest that these peptides could provide receptor-specific targeting of drugs into the pancreatic cancer cells. The prediction from the receptor-mediated accumulation of the peptides and their effects on cAMP levels was that 1a peptide should be effective with cells that express SSTR2 (and to lesser extent SSTR4 and SSTR5),



while **1b** with cells expressing any of these receptors.

Figure 3: Competition assay between **1b** and octreotide: HEK-293 cells transfected with SSTR2 or SSTR4 were pre-incubated with 800nM octreotide for 20 min, and then incubated with 400nM **1b** for 15 min, and both FITC (**1b** contains FITC moiety) (a) and RFP (b) fluorescence were monitored. (c) Merged RFP and FITC images. Phase-contrast imaging (d) was used in order to show total cell number in the samples. (e) Histogram showing quantitative image analysis of the fluorescence intensity of FITC⁺ cells (mean \pm SD; n = 10). The numbers denote mean fluorescence intensity (MFI). Data are representative of three independent experiments ($P < 0.001$).

2.3 Flow cytometry analysis on Panc-1 and Capan-1 cell lines.

The ability of the peptides **1a** and **1b** to promote drug delivery was further tested using human pancreatic cancer lines Capan-1 and Panc-1. We used flow cytometry analysis to confirm robust expression of SSTR2 and SSTR5 in these cell lines (Fig. 4). Both cell lines possess similar pattern of somatostatin receptors expression: SSTR2 was detected in 27% and 32% of cells in Panc-1 and Capan-1 consequently while SSTR5 is expressed by all cells in the population in both cell lines. In addition, 30% of Panc-1 and Capan-1 cells express both types' receptors, SSTR2 and SSTR5.

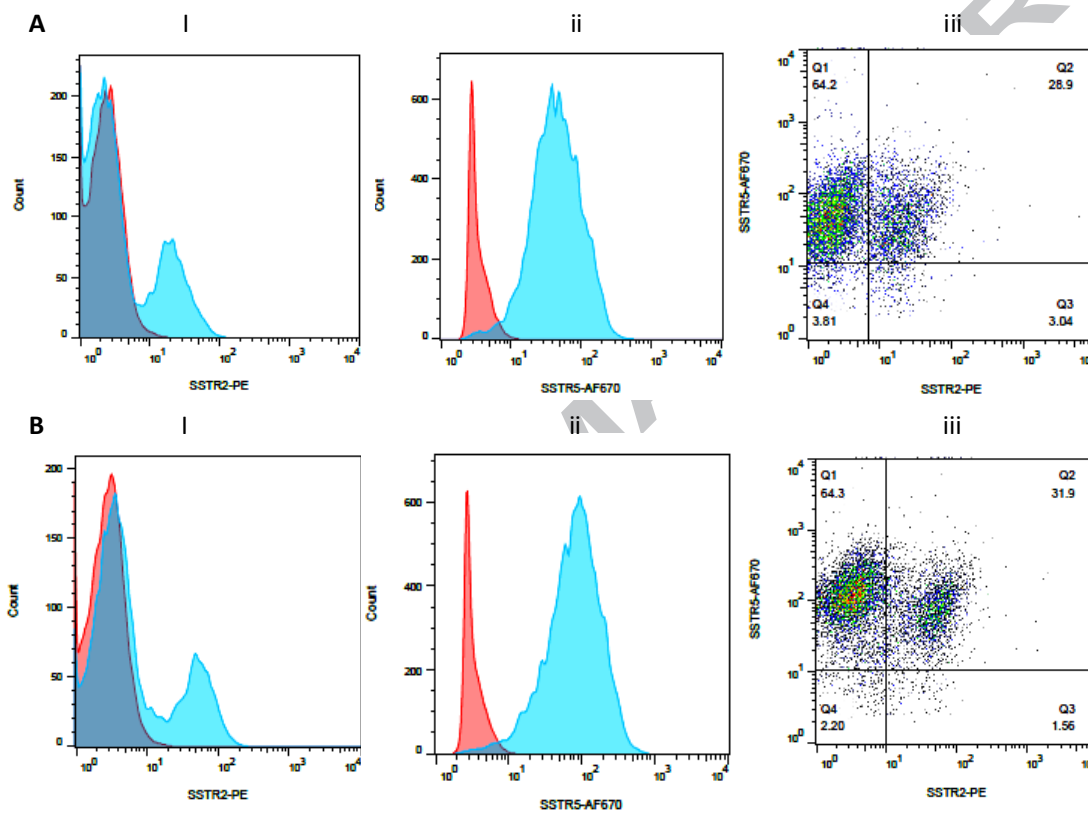


Figure 4: SSTR-2 and SSTR-5 expression in human pancreatic cancer cell lines Panc-1(A) and Capan-1(B). The cells were stained with both anti-SSTR2-PE(I) and SSTR5-AF670(II) antibodies and analysed by flow cytometry. The percentage of cells expressing both receptors is presented in III. Red: unstained cells; Aqua: cells stained with anti-SSTR2-PE(I) or SSTR5-AF670(II); Blue: Overlap between red and aqua.

Though expression of the SSTR2 and SSTR5 receptors on these cell lines was similar, Panc-1 has an inactivating mutation in SSTR5 [43], unlike Capan-1.

2.4 Peptide internalization into Panc-1 and Capan-1 cells

In spite of similar expression of the receptors in Panc-1 and Capan-1 cells, accumulation of the peptides could be very different, since it also dependent of the rate of penetration. Therefore,

we directly measure internalization of **1a** and **1b** peptides in these pancreatic lines. Cells were incubated with the fluorescent peptides, and their accumulation was monitored microscopically after the washout of the external peptides. In Panc-1 cells peptide **1a** started to show accumulation already after 5 h incubation, and the accumulation progressed during the following 19 hours. In contrast, peptide **1b** demonstrated poor internalization (Figure 5).

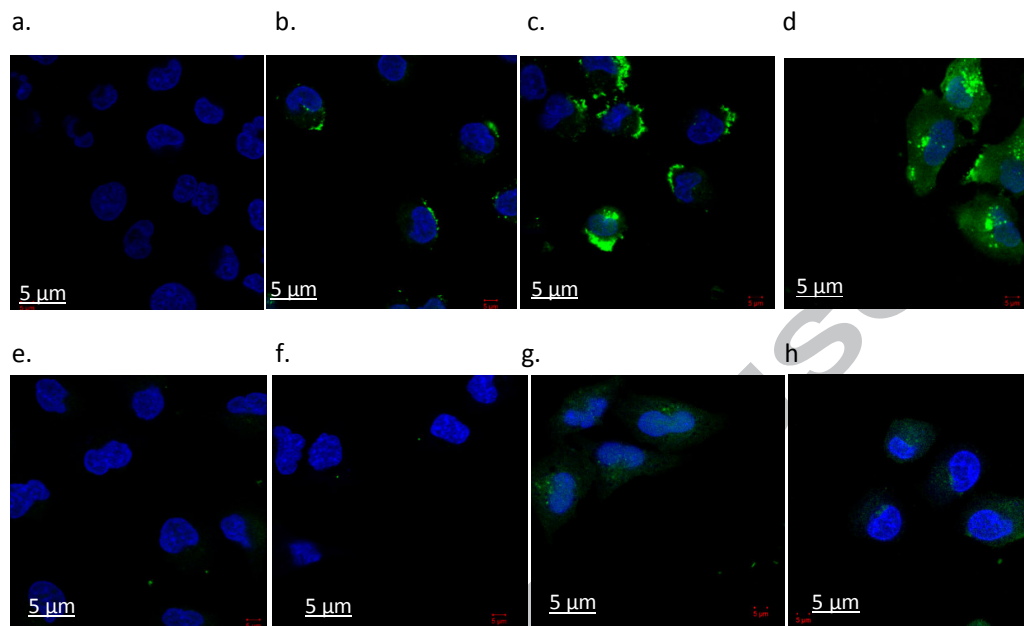


Figure 5: Confocal images of internalization of **1a** and **1b** into Panc-1 cells. Panc-1 cells were incubated with peptide FITC conjugates (green) for different time intervals Cell nuclei were stained with Dapi(blue). . For 1a: (a). 1h, (b). 5h, (c). 12h, (d). 24h (scale bar: 5 μ m each), For 1b: (e). 1h; (f). 5h; (g). 12h; (h). 24h (scale bar: 5 μ m each).

By comparison, Capan-1 cells accumulated **1a** and **1b** at similar rates (Figure 6). However, the effectiveness of accumulation was lower compared with peptide **1a** in Panc-1 cells.

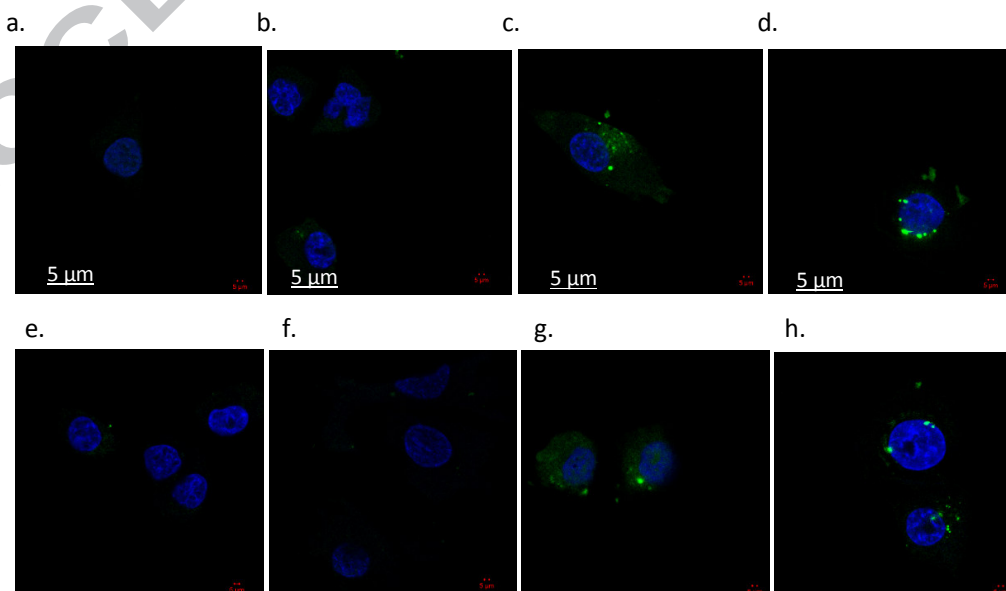


Figure 6: Confocal images of internalization of **1a** and **1b** into Capan-1 cells. Capan-1 cells were incubated with peptide FITC conjugates (green) for different time intervals. Cell nuclei were stained with Dapi(blue). For **1a**: (a). 1h, (b). 5h, (c). 12h, (d). 24h (scale bar: 5 μ m each), For **1b**: (e). 1h; (f). 5h; (g). 12h; (h). 24h (scale bar: 5 μ m each).

After making sure that peptides 1a and 1b can potentially provide specific targeting of anti-cancer drugs to pancreatic cancer cells, we evaluated conjugates of these peptides with three anti-cancer agents, including CPT, COMB and AZA, synthesized as described above.

2.5 Stability of conjugates in IMDM medium

Beside accumulation, an important factor that may affect anti-cancer activity of the drug conjugates is their stability. The stabilities of the peptide drug conjugates were measured in cell culture IMDM medium. The stability of conjugates and drug release rates varied depending on the peptide and the linked drug. Conjugates based on SSTp58 **2a** (with CPT), **3a** (with AZA) and **4a** (with COMB) ($t_{1/2}$ =3 h, $t_{1/2}$ =3 h, $t_{1/2}$ =15 h, correspondingly) decompose faster in comparison to counterpart SSTp86 **2b** (with CPT), **3b** (with AZA) and **4b** (with COMB) ($t_{1/2}$ =20 h, $t_{1/2}$ =5 h, $t_{1/2}$ =18 h, correspondingly) (Fig. 7). Nevertheless, the stabilities of both series of peptide-drug conjugates were potentially sufficient to provide potent anticancer activities. Therefore, we next tested the ability of these conjugates to kill pancreatic cancer cells in culture.

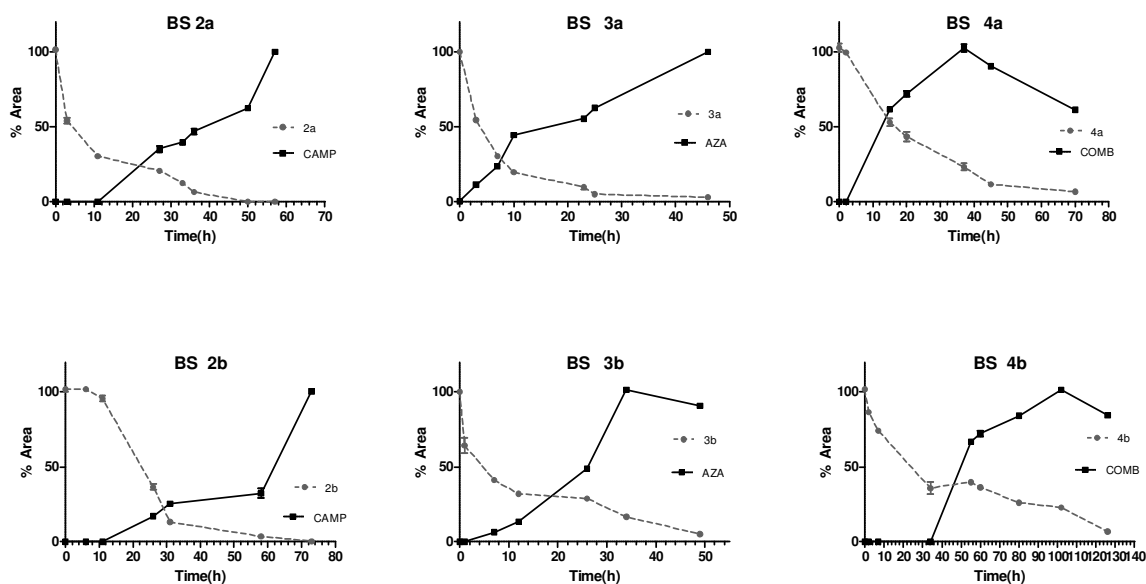


Figure 7: Biostability of peptide drug conjugates **2a-4b** in medium IMDM. Compounds were added to DME containing 20% bovine serum, amino acids and vitamins, sodium pyruvate, HEPES buffer and potassium nitrate, and incubated at a 37°C incubator for indicated time periods. Aliquots were taken and

immediately quenched with 2.5 vol of ethanol and analyzed by LC-MS. Results are given as mean \pm SD of at least three measurements.

2.6. Cell cytotoxicity of peptide conjugates

Panc-1 and Capan-1 cells were exposed to increasing doses of drugs or conjugates, and at the end of 48h or 72h incubation, metabolic activities of cells were measured using the XTT assay. Table 1 shows that peptides SSTp86 and SSTp58 alone are not cytotoxic to either cell type, while drugs alone or their conjugates with the peptides demonstrated significant toxicities.

Comp. Cell Line	SSTp58	SSTp86	2a	3a	4a	2b	3b	4b	CPT	AZA	COMB
Capan-1-48h	>50	>50	3.06 (1-8)	1.47 (0.4-5)	0.67 (0.2-2.1)	8.62 (3-27)	0.25 (0.1-6.7)	2.56 (0.8-8.1)	N/A**	1.57 (0.6-6.1)	0.84 (0.3-4.7)
Capan-1-72h	>50	>50	2.01 (0.9-7)	1.43 (0.5-5)	0.52 (0.18-1.9)	3.82 (1.4-11)	0.09 (0.03-0.34)	2.09* (0.7-9.7)	0.21 (0.07-0.66)	1.23 (0.4-4.9)	N/A**
Panc 1 48h	>50	>50	35.13 (23-65)	0.27 (0.1-0.6)	1.72 (0.5-4)	7.19* (3-15)	2.98* (1.2-7.3)	2.67 (0.13-10.4)	0.18 (0.05-0.58)	N/A**	N/A**
Panc-1-72h	>50	>50	1.71 (0.5-6)	0.14 (0.06-0.3)	1.17 (0.4-3.3)	N/A**	2.13* (0.1-5.2)	1.19 (0.06-6.3)	0.09 (0.03-0.34)	0.61 (0.2-3.8)	0.16* (0.03-0.76)

Table 1. IC₅₀ values (μ M) for SSTp58, SSTp86, 2a-b, 3a-b, 4a-b, CPT, Aza and Comb in Capan-1 and Panc-1 cell lines. IC₅₀ values were calculated using three-parameter non-linear regression. IC₅₀ values marked with * were calculated using four-parameter non-linear regression. NA** mean some fits were ambiguous and statistical comparisons of IC₅₀ curve fits (sum-of-squares F-test), IC₅₀ values and shifts could not be reliably calculated.

To our surprise, Capan-1 cells were more sensitive to 2a and 2b conjugates than Panc-1, though both cells have similar levels of SSTR2 and SSTR5 receptors. However, cytotoxic effects of peptide-drug conjugates could depend on a number of factors beside binding to receptors, including the rate of penetration, efficiency of the drug release, interaction of drugs with their targets, etc. Therefore, it is possible that for one of these reasons CAMP is more effective with Capan-1 than with Panc-1.

Notably, instability of the conjugates can lead to the release of the anti-cancer agent, which may start killing cells in culture after penetrating cells bypassing a receptor, and therefore may lead to a receptor-non-specific toxicity. Therefore, it is very difficult to make any conclusion about specific receptor-mediated anti-cancer effects of the drug conjugates based on the *in vitro* toxicity data.

Accordingly, in planning further tests we used two criteria: (a) a peptide must most effectively penetrate into cells in a receptor-specific manner, (b) the drug conjugate should show the most delayed drug accumulation due to the conjugate instability. Upon considering these criteria, we further focused on the CPT conjugates of the **a**-series of peptides, which demonstrated strong accumulation and most delayed drug release (conjugate **2a**). Furthermore, as a model for testing drug conjugate activity *in vivo*, we chose xenografts of Panc-1 cells that demonstrated the most efficient accumulation of **1a** peptide, compared to **1b** peptide and compared to **1a** peptide in Capan-1 cells. This study is currently under investigation in our lab.

2.7. *In vivo* targeting of Panc-1 tumour tissues.

To evaluate accumulation of the CPT conjugate **2a** in xenograft tumor and tissues *in vivo*, we prepared a fluorescent versions of the conjugate **1a** and **7a** (see above). Nude mice bearing 100 mm³ tumors of subcutaneously injected Panc-1 cells were intravenously administered with either the peptide **1a** (SSTp-58-FITC) or the FITC-labeled **1a**-CPT conjugate **7a** compounds. After 24 hours the compounds were found to accumulate in the tumor, though some accumulation was also seen in kidney (Fig. 8). Of note, no significant accumulation of the conjugate was seen in pancreas. Furthermore, previous studies demonstrated that fluorescein alone does not concentrate either in pancreas [44] or in tumor [45]. Therefore, accumulation in the pancreatic tumor is a specific property of the peptide-drug conjugate, which is likely to be mediated by the SSTRs

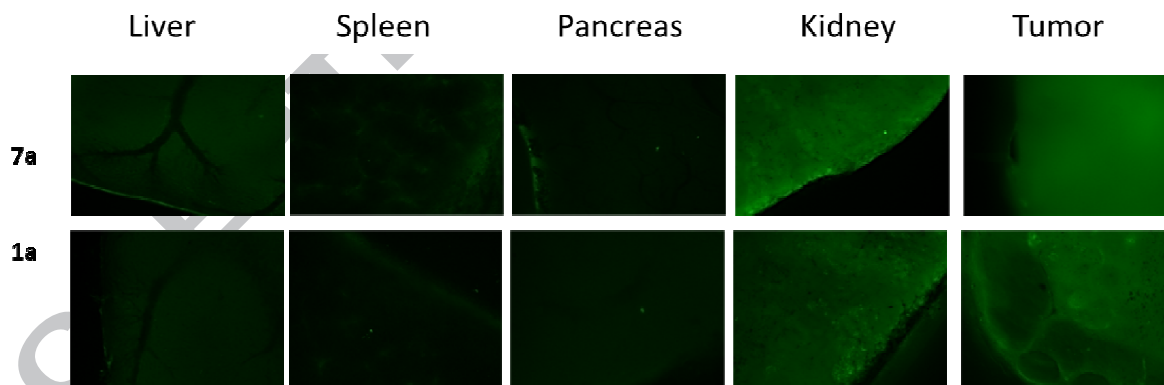


Figure 8: Tumor-specific retention of **1a** and **7a**. Panc-1 cells were injected subcutaneously into nude mice to induce a tumor. Mice bearing a 100 mm³ tumor were intravenously injected (single IP injection, 120 mg/Kg) with the fluorescent conjugates. 24 hours post injection the tumor, spleen, pancreas, kidney and the liver were excised and evaluated for accumulation of fluorescence microscopically.

These data suggested that the peptide **1a**-CPT (namely **2a**) drug conjugate could show specific inhibitory effects against pancreatic cancer.

3. Conclusions

Here we designed cyclic peptide that interact with wide range of somatostatin receptors present in pancreatic cancer cells and in human pancreatic tumors. These peptides penetrate cells *via* receptor-mediated mechanisms and selectively deliver anti-cancer drugs to pancreatic tumors in a xenograft model. The peptide-drug conjugates demonstrate strong activity against pancreatic cancer. Therefore, this approach lay the basis for development of novel drugs against pancreatic cancer.

4. Materials and Methods

4.1 Reagents and cell lines

Camptothecin (CPT), all protected amino acids, resin and coupling reagents were purchased from **Tzamal D-Chem Laboratories Ltd.** Petah-Tikva, Israel. Combretastatin 4A (COMB) [33] and Azatoxin (AZA) [34] were synthesized according to the literature procedures. All the solvents were purchased from Bio-Lab Ltd. Jerusalem, Israel or Gas Technologies Ltd. Kefar Saba, Israel. All other chemicals including IMDM medium were purchased from Holland Moran or Sigma-Aldrich. All the cell lines were cultured in an RPMI medium supplemented with 2 mM glutamine, 10% fetal bovine serum and with penicillin streptomycin (100 IU/ml of each). (The cell culture growth medium and all of its additives were purchased from Biological Industries, Bet-Ha'emek, Israel). All cell cultures were grown at a 37°C incubator in an environment containing 6% CO₂. The cytotoxicity of the materials was determined by measuring the mitochondrial enzyme activity, using a commercial XTT assay kit (Biological Industries, Bet-Ha'emek, Israel). All samples contained DMSO at final concentration <0.05%. All the cancer cell lines were kindly provided by Prof. Arie Ornstein (Sheba Medical Center, Israel). Noncancerous HEK-293 were obtained from the American Type Culture Collection (ATCC, Manassas, VA, USA).

4.2 High performance liquid chromatography (HPLC)

All HPLC purifications were done via reverse phase on ECOM semi-preparative system with dual UV detection at 254 and 214 nm. Phenomenex Gemini® 10 µm C18 110 Å, LC 250 x 21.2 mm prep column was utilized. The column was kept at room temperature. The eluent solvents were 0.1% TFA in H₂O (A) and 0.1% TFA in ACN (B). A typical elution was a

gradient of 100% A to 50% B over 45 min at a flow rate of 25 mL/min. Analytical RP-HPLC was performed on an UltiMate 3000 system (Dionex) using a Vydac C18 column (250 x 4.6 mm) with 5 μm silica (300 \AA pore size). Linear gradient elution (0 min 0% B; 5 min 0% B; 50 min 90% B) with eluent A (0.1% TFA in water) and eluent B (0.1% TFA in acetonitrile: H₂O (80:20, v/v)) was used at a flow rate of 1 mL/min.

4.3 Liquid Chromatography Mass Spectrometry (LCMS)

Electron spray mass spectra (ESI-MS) were obtained using an Autoflex III smart-beam (MALDI, Bruker), Q-TOF micro (Waters) or an LCQ FleetTM ion trap mass spectrometer (Finnigan/Thermo). HPLC/LC-MS analyses were made using Agilent infinity 1260 connected to Agilent quadruple LC-MS 6120 series equipped with ZORBAX SB-C18, 2.1 x 50mm, 1.8 μm column. In all cases the eluent solvents were A (0.1% FA in H₂O) and B (0.1% FA in ACN) and the elution gradient profile was: 100% A for first 3 min, followed by 5 min (from min 3 to min 8) during which it reached 100% B, followed by 5 min (from min 8 to min 13) of 100% B, followed by two min (from min 13 to min 15) during which it returned back to A, followed by 2 min (from min 15 to min 17) of 100% A. The UV detection was at 254 nm. The column temperature was kept at 50⁰C. The flow rate was of 0.3 ml /min. The MS fragmentor was tuned on 30V or 70V on positive or negative mode.

4.4 Synthesis of Peptide- mono-Drug conjugates 1-4.

Coupling step: The synthesis of all the cyclic conjugates **1-4** were provided using previously described procedure [15, 35]. For more detailed procedures see supplementary material. Briefly, in a reaction vessel equipped with a sintered glass bottom, rink amide MBHA resin, (substitution level 0.56mmol/g, 1g) was swelled in NMP by agitation overnight. The Fmoc group was removed from the resin upon treatment with 20% piperidine in NMP (10ml) for 15 min. This action was repeated twice. After washing the resin with NMP (7 times, 10 ml, 2 min each time), Fmoc-GlyS2(Acm)-OH [28] building unit (3 eq, 10.5 mmol, 0.64 g) dissolved in NMP (7 ml) was activated with PyBoP (3 eq, 10.5 mmol, 0.7 g) and DIEA (6 eq, 21 mmol, 0.521 ml) for 4 min at room temperature, transferred to the reaction vessel and allowed to react for 1h at rt. Following coupling, the peptidyl resin was washed with NMP (5 times, 7 ml) for 2 min each time, completion of reaction was monitored by ninhydrin test (Kaiser test, yellow), The deblock mixture was a mixture of 80:20 DMF/piperidine (v/v).

Cyclization step: After coupling of Fmoc-Cys(Acm)-OH and NMP wash, the resin was washed with 4:1 DMF/water (3 times, 6.5 ml, 2min each time). A solution of I₂ (10eq, 35 mmol, 1.29 g) in 4:1 DMF/water (10 ml) was added to the peptidyl – resin followed by agitation at rt for 1h

to afford the disulfide bridge cyclization [37]. The peptidyl – resin was filtered and washed extensively with 4:1 DMF/water (7 times, 10 ml, 2 min each time), DMF (6 times, 10 ml, 2 min each time), DCM (6 times, 10 ml, 2 min each time), CHCl_3 (4 times, 10 ml, 2 min each time), 2% ascorbic acid in DMF (6 times, 10 ml, 2 min each time) and last wash with DMF (6 times, 10 ml, 2 min each time). Finally, coupling of last amino acid Fmoc-D-Phe-OH after cyclization, gave cyclic peptides.

Coupling of Fmoc-g-aminobutyric acid (linker): Fmoc-g-aminobutyric acid (3eq, 10.5mmol, 0.49 g) dissolved in NMP (7 ml) was activated with PyBroP (3 eq, 10.5 mmol, 0.7 g) and DIEA (6 eq, 21mmol, 0.521 ml) for 4 min at room temperature, transferred to the reaction vessel and allowed to react for 1h at rt. After post coupling wash and Fmoc-deprotection the peptidyl resin is ready for drug conjugation.

Coupling of anticancer agents to 5a and 5b: The peptidyl resin was washed and a DMF/DCM (1:1) and solution of premade 4-nitrophenylcarbonate derivative of CPT, AZA and COMB (anticancer agent (1.2 eq.), 4-nitrophenyl chloroformate (1.2 eq.), DMAP (1.2 eq.), DIPEA (3 eq.) in DCM, 3h, rt) of was added to the exposed primary amine for overnight at rt, leading to the corresponding carbamate conjugation site. The resin was thoroughly washed (DCM, NMP, 2 x DCM) and the peptide conjugate was cleaved from the polymeric support with the cold TFA/TIS/ H_2O (95:2.5:2.5) cocktail. The solvents were removed under a gentle flow of N_2 and then the crude was precipitated from diethyl ether. The supernatant centrifuged and dried by lyophilization. The purification was conducted on semi-preparative HPLC (AcCN, 0.1% TFA in H_2O) led to final conjugates with carbamate linkage **2a-b**, **3a-b** and **4a-b** correspondingly. For **2a**: (42% yield) LC-MS: RT = 8.25 min; ESI-MS m/z calcd: 854.3 found: 854.8 (M/2+H), calcd: 569.9 found: 570.2 (M/3+H); For **2b**: (41% yield) LC-MS: RT = 9.04 min; HRMS (ESI-MS): m/z calcd: 1759.691 found: 1759.679 (M+Na) For **3a**: (38% yield) LC-MS: RT = 8.57 min; ESI-MS m/z calcd: 871.37 found: 871.0 (M/2+2H), calcd: 580.5 found: 580.9 (M/3+H). For **3b**: (36% yield) LC-MS: RT = 9.17 min; ESI-MS m/z calcd: 885.36 found: 885.0 (M/2+H). For **4a**: (32% yield) LC-MS: RT = 8.18 min; HRMS: ESI-MS m/z calcd: 839.37 found: 839.5 (M/2+2H), calcd: 560.2, found: 560.1 (M/3+2H). For **4b**: (43% yield) LC-MS: RT = 9.76 min; HRMS (ESI-MS): m/z calcd: 1705.718 found: 1705.739 (M+H), calcd: 1727.713, found: 1727.716 (M+Na).

4.5 Synthesis of hetero peptide conjugates **7a,b**.

To the intermediates **5a** and **5b**, Fmoc-Lys(Dde)-OH was coupled to the primary amine using standard coupling procedure (PyBoP, DIEA in NMP) with 2-fold excess of the AA, leading to

resin bound **6a** and **6b** (Scheme 3). Initially, the Fmoc group was removed (7 ml of 20% piperidine in DMF, 10 min, 2 cycles) and the deblocked *N*-terminus amine was reacted with the preactivated form of CPT by the procedure mentioned above for **2a,b**. Then, Dde was removed by three cycles of 2% hydrazine in 7 ml DMF, 3 min each and after washing the primary ω -amine of Lys was allowed to react with FITC (FITC, 1.5 eq., DIEA, 3 eq. in 7 ml DMF). Finally, the on-resin synthesized conjugates were cleaved from the solid support in the same manner as for **2-4** and precipitated by the addition of cold diethyl ether, isolated (centrifugation), lyophilized, purified (HPLC, AcCN, 0.1% TFA in H₂O) and identified by LC-MS and HRMS as dual conjugates **7a-b**. **7a** 40% yield. LC-MS: RT = 9.86 min; MS: ESI-MS *m/z* calcd: 2226.9, found: 1113.8 (M/2+2H), calcd: 742.28, found: 742.8 (M/3+1H). **7b** 38% yield. LC-MS: RT 10.08 min; MS: ESI-MS *m/z* calcd: 1127.92 (M/2+2H), found: 1128.87 (M/2+2H).

4.6 cAMP signaling pathway activity assessment

cAMP signaling pathway activity was assessed using reporter gene system of the cAMP response element (CRE) fused to firefly luciferase [36]. 70,000 HEK-293 cells were seeded in 24 well plates and a day later the cells were co-transfected with CRE-luciferase reporter plasmid, β -galactosidase expression construct and with SSTR 1-5 expression vectors or with control empty vector (pcDNA3.1). Transfections were carried out with JetPei transfection reagent (Polyplus-transfection, NY, USA) according to the manufacturer's recommendation. After 1 day cells were treated with forskolin (FSK) 10 μ M or FSK plus SST analog. Forskolin-induced CRE promoter activity inhibition by SSTRs agonists was evaluated by monitoring luminescence, assessed relative to FSK alone and normalized to β -galactosidase activity calculated by ONPG/ beta GAL assay [37, 38]. Experiments were conducted in triplicates. The data shown are representative of three experiments.

4.7 Bio-stability in IMDM Medium

This medium is a modification of Dulbecco's Modified Eagle's Medium (DME) containing 20% bovine serum, amino acids and vitamins, sodium pyruvate, HEPES buffer and potassium nitrate. Incubation procedure: Incubations were conducted at a 37°C incubator with 1 ml IMDM medium per incubation tube. The samples were prepared by adding 10 μ l of stock solution (see below) to the medium at the beginning of the incubation period. Aliquots of the incubation mixture were removed after 1, 3, 6, 24, 48, 72 and 96 h and then immediately quenched with 2.5 vol of ethanol. The samples were centrifuged at 14000 rpm for 15 min. Supernatants were collected, filtered and analyzed by LC-MS.

4.8 Cytotoxicity test

The cytotoxicity of the peptide-drug conjugates was determined by measuring the mitochondrial enzyme activity, using a commercial XTT assay kit. All samples contained DMSO at final concentration <0.05%. Cells were cultured in micro wells at $5-10 \times 10^4$ cells/mL and incubated for 24 h, 48h, and 72h. After the first incubation period the cultures were washed and then given a fresh medium containing different concentrations of the tested substances. At the end of the second incubation, XTT reagent was added and the cells were re-incubated for additional 2-4 h. During that time the absorbencies in the wells were measured with a TECAN Infinite M200 ELISA reader at both 480 and 680nm. The difference between these measurements was used for calculating the % Growth Inhibition (GI) in test wells compared to two controls: cells that were exposed to the medium and solvent, and those which were exposed to a solvent-free medium. All the tests were done in tetra-plicate. Each experiment was conducted twice.

4.9 Direct immunofluorescence assay and flow cytometry

For evaluating SSTR2 and SSTR5 expression the Panc-1 and Capanc-1 cells were washed with PBS and scrapped from the culture flask. 10^6 of cells were incubated with 10 μ L of ready for use Anti-Human Somatostatin R2/SSTR2-PE and Anti-Human Somatostatin R5/SSTR5-Alexa Fluor 647 that specifically binds SSTR2 and SSTR5 correspondingly (FAB4224P, IC4448RBD Bioscience, San Jose, CA, USA) at 4°C for 45 min for the antibody. Following two washings with PBS the cells were re-suspended in 400 μ L of PBS and analyzed with Becton Dickson FACS Calibur cell analyzer equipped with an argon-ion laser (15W) at 488 nm with a 637 DF filter. For each sample $\sim 10^4$ cell were analyzed. FlowJo software was used to analyze the collected data. For background measurement, the cells were treated at the same conditions but without adding the antibody.

4.10 Fluorescent microscopy on non-cancerous HEK-293: Binding affinity assay

70,000 HEK-293 cells were seeded in 24 well plates and a day later the cells were co-transfected with SSTR 1-5 expression vectors or with control empty vector (pcDNA3.1) and with an RFP expression vector, in order to confirm successful transfection and correct imaging. Transfections were carried out as described above. After 1 day the cells were passaged at \approx 30% confluence and a day later the cells were incubated with FITC-labeled peptide **1b** in serum-free DMEM for 30 min. Peptide accumulation was examined by fluorescence microscopy (cell[^]R-Imaging Station, Olympus IX2-ZDC, Hamburg, Germany).

4.11 Confocal microscopy on cancer cell lines

For confocal microscopy analysis, the cells were treated with two different peptides **1a** and **1b** and subjected to accumulation in different period of time, the images were collected with a Zeiss LSM700 confocal microscope.

4.12 Ex vivo fluorescent imaging on cancer cell lines

Five-week-old athymic nude mice (Harlan Labs, Nes Ziona, Israel) were subcutaneously inoculated in the dorsal left side with Panc-1 cells, and tumors allowed to establish over time. When tumor volume reached 100 mm³, **1a** and **7a** (120 mg/kg) was intravenously administered. After 24 hours, fluorescent images of **1a** and **7a** were acquired by Photometrics CoolSNAP HQ2 camera mounted on an Olympus iX81 fluorescent microscope.

Acknowledgements

The authors thank Prof. Dan Meyerstein from the Department of Chemical Sciences, Ariel University for technical support and fruitful advices in performing mass spectroscopy. The authors also thank Mrs. Cherna Moskowitz for generous stipend to E.R. Financial support was provided by Ariel University Internal Research and Development Program (ASI-GG-2017-004).

Appendix A. Supplementary data

Supplementary data related to this article can be found at:

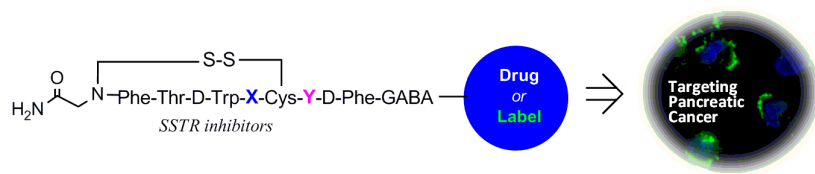
References

1. Siegel, R. L., Miller, K. D., Jemal, A. **2015** Cancer statistics, 2015. *CA: a cancer journal for clinicians* 65, 5-29
2. Bobrov, E., Skobeleva, N., Restifo, D., Beglyarova, N., Cai, K. Q., Handorf, E., Campbell, K., Proia, D. A., Khazak, V., Golemis, E. A., Astsaturov, I. **2017** Targeted delivery of chemotherapy using HSP90 inhibitor drug conjugates is highly active against pancreatic cancer models. *Oncotarget* 8, 4399-4409
3. Dubey, R. D., Alam, N., Saneja, A., Khare, V., Kumar, A., Vaidh, S., Mahajan, G., Sharma, P. R., Singh, S. K., Mondhe, D. M., Gupta, P. N. **2015** Development evaluation of folate functionalized albumin nanoparticles for targeted delivery of gemcitabine. *International journal of pharmaceutics* 492, 80-91
4. Khare, V., Alam, N., Saneja, A., Dubey, R. D., Gupta, P. N. **2014** Targeted drug delivery systems for pancreatic cancer. *Journal of biomedical nanotechnology* 10, 3462-3482
5. Khare, V., Singh, A., Mahajan, G., Alam, N., Kour, S., Gupta, M., Kumar, A., Singh, G., Singh, S. K., Saxena, A. K., Mondhe, D. M., Gupta, P. N. **2016** Long-circulatory nanoparticles for gemcitabine delivery: Development investigation of pharmacokinetics and in-vivo anticancer efficacy. *European*

6. Yoshida, M., Takimoto, R., Murase, K., Sato, Y., Hirakawa, M., Tamura, F., Sato, T., Iyama, S., Osuga, T., Miyanishi, K., Takada, K., Hayashi, T., Kobune, M., Kato, J. **2012** Targeting anticancer drug delivery to pancreatic cancer cells using a fucose-bound nanoparticle approach. *PloS one* 7, e39545
7. Parsian, M., Unsoy, G., Mutlu, P., Yalcin, S., Tezcaner, A., Gunduz, U. **2016** Loading of Gemcitabine on chitosan magnetic nanoparticles increases the anti-cancer efficacy of the drug. *European journal of pharmacology* 784, 121-128
8. Yang, F., Jin, C., Jiang, Y., Li, J., Di, Y., Ni, Q., Fu, D. **2011** Liposome based delivery systems in pancreatic cancer treatment: from bench to bedside. *Cancer treatment reviews* 37, 633-642
9. Spring, B. Q., Bryan Sears, R., Zheng, L. Z., Mai, Z., Watanabe, R., Sherwood, M. E., Schoenfeld, D. A., Pogue, B. W., Pereira, S. P., Villa, E., Hasan, T. **2016** A photoactivable multi-inhibitor nanoliposome for tumour control and simultaneous inhibition of treatment escape pathways. *Nature nanotechnology* 11, 378-387
10. Lee, K. H., Galloway, J. F., Park, J., Dvoracek, C. M., Dallas, M., Konstantopoulos, K., Maitra, A., Searson, P. C. **2012** Quantitative molecular profiling of biomarkers for pancreatic cancer with functionalized quantum dots. *Nanomedicine : nanotechnology, biology, and medicine* 8, 1043-1051
11. Khare, V., Sakarchi, W. A., Gupta, P. N., Curtis, A. D. M., Hoskins, C. **2016** Synthesis and characterization of TPGS-gemcitabine prodrug micelles for pancreatic cancer therapy. *RSC Advances* 6, 60126-60137
12. Ahn, J., Miura, Y., Yamada, N., Chida, T., Liu, X., Kim, A., Sato, R., Tsumura, R., Koga, Y., Yasunaga, M., Nishiyama, N., Matsumura, Y., Cabral, H., Kataoka, K. **2015** Antibody fragment-conjugated polymeric micelles incorporating platinum drugs for targeted therapy of pancreatic cancer. *Biomaterials* 39, 23-30
13. Gilad Y, Firer M, Gellerman G. Recent Innovations in Peptide Based Targeted Drug Delivery to Cancer Cells. *Biomedicines*. 2016;4(2):11.
14. Firer, M. A., Gellerman, G. **2012** Targeted drug delivery for cancer therapy: the other side of antibodies. *Journal of hematology & oncology* 5, 70
15. Gilad, Y., Noy, E., Senderowitz, H., Albeck, A., Firer, M. A., Gellerman, G. **2015** Dual-drug RGD conjugates provide enhanced cytotoxicity to melanoma and non-small lung cancer cells. *Peptide Science* 106 (2), 160-171
16. Wang, Y., Cheetham, A. G., Angacian, G., Su, H., Xie, L., Cui, H. **2017** Peptide-drug conjugates as effective prodrug strategies for targeted delivery. *Advanced drug delivery reviews* 110-111, 112-126
17. Aggarwal, S., Ndinguri, M. W., Solipuram, R., Wakamatsu, N., Hammer, R. P., Ingram, D., Hansel, W. **2011** [DLys(6)]-luteinizing hormone releasing hormone-curcumin conjugate inhibits pancreatic cancer cell growth in vitro and in vivo. *International journal of cancer* 129, 1611-1623
18. Sun, L. C., Coy, D. H. **2011** Somatostatin receptor-targeted anti-cancer therapy. *Current drug delivery* 8, 2-10
19. Papotti, M., Bongiovanni, M., Volante, M., Allia, E., Landolfi, S., Helboe, L., Schindler, M., Cole, S. L., Bussolati, G. **2002** Expression of somatostatin receptor types 1-5 in 81 cases of gastrointestinal and pancreatic endocrine tumors. A correlative immunohistochemical and reverse-transcriptase polymerase chain reaction analysis. *Virchows Archiv : an international journal of pathology* 440, 461-475
20. Reubi, J. C., Schaer, J. C., Laissue, J. A., Waser, B. **1996** Somatostatin receptors and their subtypes in human tumors and in peritumoral vessels. *Metabolism: clinical and experimental* 45, 39-41
21. Denzler, B., Reubi, J. C. **1999** Expression of somatostatin receptors in peritumoral veins of human tumors. *Cancer* 85, 188-198
22. Li, M., Li, W., Kim, H. J., Yao, Q., Chen, C., Fisher, W. E. **2004** Characterization of somatostatin receptor expression in human pancreatic cancer using real-time RT-PCR. *The Journal of surgical research* 119, 130-137

23. Kikutsuji, T., Harada, M., Tashiro, S., Ii, S., Moritani, M., Yamaoka, T., Itakura, M. **2000** Expression of somatostatin receptor subtypes and growth inhibition in human exocrine pancreatic cancers. *Journal of hepato-biliary-pancreatic surgery* 7, 496-503
24. Shahbaz, M., Ruliang, F., Xu, Z., Benjia, L., Cong, W., Zhaobin, H., Jun, N. **2015** mRNA expression of somatostatin receptor subtypes SSTR-2, SSTR-3, and SSTR-5 and its significance in pancreatic cancer. *World journal of surgical oncology* 13, 46
25. Grozinsky-Glasberg, S., Grossman, A. B., Korbonits, M. **2008** The role of somatostatin analogues in the treatment of neuroendocrine tumours. *Molecular and cellular endocrinology* 286, 238-250
26. Sun, L., Fuselier, J. A., Coy, D. H. **2004** Effects of camptothecin conjugated to a somatostatin analog vector on growth of tumor cell lines in culture and related tumors in rodents. *Drug delivery* 11, 231-238
27. Lelle, M., Kaloyanova, S., Freidel, C., Theodoropoulou, M., Musheev, M., Niehrs, C., Stalla, G., Peneva, K. **2015** Octreotide-Mediated Tumor-Targeted Drug Delivery via a Cleavable Doxorubicin-Peptide Conjugate. *Molecular pharmaceuticals* 12, 4290-4300
28. Gazal, S., Gellerman, G., Glukhov, E., Gilon, C. **2001** Synthesis of novel protected Nalpha(omega-thioalkyl) amino acid building units and their incorporation in backbone cyclic disulfide and thioetheric bridged peptides. *The journal of peptide research : official journal of the American Peptide Society* 58, 527-539
29. Kostenich, G., Oron-Herman, M., Kimel, S., Livnah, N., Tsarfay, I., Orenstein, A. **2008** Diagnostic targeting of colon cancer using a novel fluorescent somatostatin conjugate in a mouse xenograft model. *International journal of cancer* 122, 2044-2049
30. Kostenich, G., Livnah, N., Bonasera, T. A., Yechezkel, T., Salitra, Y., Litman, P., Kimel, S., Orenstein, A. **2005** Targeting small-cell lung cancer with novel fluorescent analogs of somatostatin. *Lung cancer (Amsterdam, Netherlands)* 50, 319-328
31. Colucci, R., Blandizzi, C., Ghisu, N., Florio, T., Del Tacca, M. **2008** Somatostatin inhibits colon cancer cell growth through cyclooxygenase-2 downregulation. *British journal of pharmacology* 155, 198-209
32. Taylor, J. E., Theveniau, M. A., Bashirzadeh, R., Reisine, T., Eden, P. A. **1994** Detection of somatostatin receptor subtype 2 (SSTR2) in established tumors and tumor cell lines: evidence for SSTR2 heterogeneity. *Peptides* 15, 1229-1236
33. Parihar, S., Kumar, A., Chaturvedi, A. K., Sachan, N. K., Luqman, S., Changkija, B., Manohar, M., Prakash, O., Chanda, D., Khan, F., Chanotiya, C. S., Shanker, K., Dwivedi, A., Konwar, R., Negi, A. S. **2013** Synthesis of combretastatin A4 analogues on steroidal framework and their anti-breast cancer activity. *The Journal of steroid biochemistry and molecular biology* 137, 332-344
34. Cline, S. D., Macdonald, T. L., Osheroff, N. **1997** Azatoxin is a mechanistic hybrid of the topoisomerase II-targeted anticancer drugs etoposide and ellipticine. *Biochemistry* 36, 13095-13101
35. Redko, B., Ragozin, E., Andreii, B., Helena, T., Amnon, A., Talia, S. Z., Mor, O. H., Genady, K., Gary, G. **2015** Synthesis, drug release, and biological evaluation of new anticancer drug-bioconjugates containing somatostatin backbone cyclic analog as a targeting moiety. *Biopolymers* 104, 743-752
36. George, S. E., Bungay, P. J., Naylor, L. H. **1997** Evaluation of a CRE-Directed Luciferase Reporter Gene Assay as an Alternative to Measuring cAMP Accumulation. *Journal of biomolecular screening* 2, 235-240
37. Møller, L. N., Stidsen, C. E., Hartmann, B., Holst, J. J. **2003** Somatostatin receptors. *Biochimica et Biophysica Acta (BBA) - Biomembranes* 1616, 1-84
38. Miller, J. H. **1972** *Experiments in molecular genetics*, Cold Spring Harbor Laboratory, Cold Spring Harbor, N.Y.
39. Patel, Y. C., Greenwood, M. T., Warszynska, A., Panetta, R., Srikant, C. B. **1994** All five cloned human somatostatin receptors (hSSTR1-5) are functionally coupled to adenylyl cyclase. *Biochemical and biophysical research communications* 198, 605-612
40. Tentler, J. J., Hadcock, J. R., Gutierrez-Hartmann, A. **1997** Somatostatin acts by inhibiting the cyclic 3',5'-adenosine monophosphate (cAMP)/protein kinase A pathway, cAMP response element-binding

- protein (CREB) phosphorylation, and CREB transcription potency. *Molecular endocrinology (Baltimore, Md.)* 11, 859-866
41. Williams, C. **2004** cAMP detection methods in HTS: selecting the best from the rest. *Nature reviews. Drug discovery* 3, 125-135
 42. Malik, R., Bora, R. S., Gupta, D., Sharma, P., Arya, R., Chaudhary, S., Saini, K. S. **2008** Cloning, stable expression of human phosphodiesterase 7A and development of an assay for screening of PDE7 selective inhibitors. *Applied microbiology and biotechnology* 77, 1167-1173
 43. Zhou, G., Gingras, M. C., Liu, S. H., Li, D., Li, Z., Catania, R. L., Stehling, K. M., Li, M., Paganelli, G., Gibbs, R. A., Demayo, F. J., Fisher, W. E., Brunicardi, F. C. **2011** The hypofunctional effect of P335L single nucleotide polymorphism on SSTR5 function. *World journal of surgery* 35, 1715-1724
 44. Kuneš M., Květina J., Maláková J., Bureš J., Kopáčová M., Rejchrt S. **2010** Pharmacokinetics and organ distribution of fluorescein in experimental pigs: an input study for confocal laser endomicroscopy of the gastrointestinal tract. *Neuroendocrinol Lett*; 31(Suppl.2):101–105
 45. Redko B., Tuchinsky H., Segal T., Tobi D., Luboshits G., Pinhasov A., Gerlitz G., Gellerman G. **2017** Toward the development of a novel non-RGD cyclic peptide drug conjugate for treatment of human metastatic melanoma. *Oncotarget*, 8(1), 757-768
 46. Chen X., Zhang X-Y., Shen Y., Fan L-L., Ren M-L., Wu Y-P. Synthetic paclitaxel-octreotide conjugate reversing the resistance of A2780/Taxol to paclitaxel in xenografted tumor in nude mice. **2016** *Oncotarget*, 7, 83451-83461
 47. Huang C-M., Wu Y-Ta., Chen S-T. Targeting delivery of paclitaxel into tumor cells via somatostatin receptor endocytosis. **2000**, *Chem. & Biol.*, 7, 453–461.



ACCEPTED MANUSCRIPT

Highlights

- New cyclic peptide-drug conjugates for effective targeting pancreatic cancer were discovered.
- These conjugates comprising cyclic peptides SSTp-58 and SSTp-86 that are based on the sandostatin motive.
- The drug conjugates specifically accumulated in tumors in the animal xenograft model.

ACCEPTED MANUSCRIPT